Egypt. J. Anal. Chem., Vol. 17, pp. 1- 11.(2008)

Synthesis and Characterization of New bis Salicylidene Adipic Hydrazones and their Metal Chelates with Mn^{2+}, Co^{2+}, Ni^{2+}, Cu^{2+} and Zn^{2+}

Said A. Amer, Ikhlas A. Mansour, Raafat M. Issa and Abdel-Monsef I. Abdel-Monsef

Chemistry Department - Faculty of Science - Tanta University- Tanta- Egypt
E-mail: Said_anwer@yahoo.com

Summary: Dibasic tetradentate adipic dihydrazones were synthesized and characterized, their metal chelates of Mn^{2+}, Co^{2+}, Ni^{2+}, Cu^{2+} and Zn^{2+} were prepared in MeOH using salicylidene adipic dihydrazone and dihydroxy benzylidene adipic dihydrazone. On the basis of various physical properties, the complexes can be described as having four coordinate tetrahedral and square planar geometry. The solid state ESR spectra of Mn^{2+}, Co^{2+} and Cu^{2+} complexes show broad signals which result from the spin-spin interaction between two M(II) ions existing in the binuclear M(II) complexes; this is in accordance with the results of magnetic moments.

Introduction

Much work has been done on the biological activity of hydrazones[1,2]. Most of these hydrazones are of special interest due to their use in the treatment of diseases such as tuberculosis, leprosy and mental disorder[3]. Their influence has been attributed to the formation of stable complexes with the metal ions present in the cell[4]. The chemistry of hydrazones and their derivatives has received considerable attention due to their application as complexing agents[5,6]. Coordination compounds of aroyl hydrazones with transition metal ions have been reported to act as enzyme inhibitors[7] and have useful pharmacological applications[8]. Recently, an increasing number of metal complexes of hydrazones have been studied[9,10], particularly, those of palladium(II), platinum(II) and rhodium(II) which were reported to have potential antitumor activity[11,12].

In this paper we describe the synthesis and characterization of transition metal ion complexes based on Schiff bases derived from condensing adipic dihdrazide with salicylaldehyde H_4L^1 or 2,5-dihydroxy benzaldehyde H_4L^2 (Scheme I).

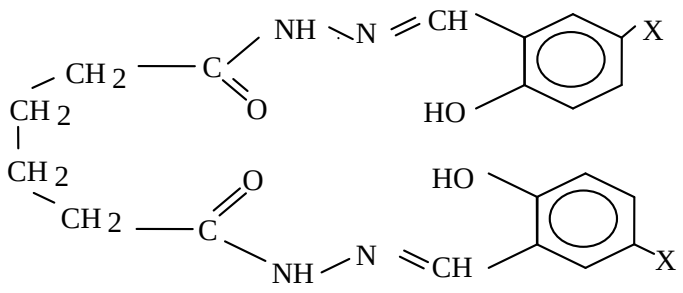

X = H H_4L^1
X = OH H_4L^2

Scheme I

Experimental

All chemicals and solvents were reagent grade commercial materials and were used as received.

1- Preparation of adipic dihydrazones

The ligands used in the present investigation are salicylidene adipic dihydrazone H_4L^1 and 2,5-dihydroxy-benzylidene adipic dihydrazone H_4L^2. These were prepared by mixing adipic dihydrazide with salicylaldehyde or 2,5-dihydroxy benzaldehyde in ratio of 1:2 mole in absolute methanol and stirring for 2 hours. The reaction products were filtered off, crystallized from methanol and finally dried in a vacuum desiccator over anhydrous $CaCl_2$.

2- Preparation of the metal complexes of adipic dihydrazones.

Metal acetates of the divalent ions Mn^{2+}, Co^{2+}, Ni^{2+}, Cu^{2+}, Zn^{2+} were mixed in (2:1) mole ratios with the prepared ligands H_4L^1, H_4L^2 in absolute methanol. The reaction mixture was refluxed on a water bath for 5 hours. The formed complexes were filtered off, washed several times with pure dry methanol and dried in vacuo over anhydrous $CaCl_2$.

The C, H and N analyses were determined at the microanalytical center of Cairo University, Egypt. The IR spectra were measured as KBr discs using a Perkin-Elmer 1430 infrared spectrometer (4000-200 cm^{-1}). Electronic absorption

spectra in the 200-900 nm region were recorded on a Perkin-Elmer 550 spectrophotometer.

The thermal analyses (DTA and TGA) were carried out on a Shimadzu DT-30 and TG-50 thermal analyzers within the temperature range 27-800 ^{o}C. The magnetic susceptibilities were measured at room temperature using the Gouy method with mercuric tetrathiocyanatocobaltate (II) as magnetic susceptibility standard. Diamagnetic corrections were made using Pascal's constants[13]. Magnetic susceptibilities were measured using the equation: $\mu_{eff} = 798\text{-} (\chi_m T)^{1/2}$.

Solid state powder X-band ESR measurements at room temperature were carried out using Joel spectrometer model JES-FE 2XG equipped with an E101 microwave bridge. DPPH was used as the standard material.

Results and Discussion

The analytical data of the ligands and their complexes with physical properties are summarized in Table 1. The analytical data correspond well with the general formula $[M_2(H_2L)(AcO)_2]_2.nH_2O$ where M = Mn^{2+}, Co^{2+}, Ni^{2+}, Cu^{2+}, Zn^{2+}, L = H_4L^1 or H_4L^2 and n= 4 for complex (4), 3 for complex (8) and 1 for all other complexes.

Thermal analysis

The compounds under investigation were subjected to thermal (DTA & TGA) analysis in order to confirm the nature and number of water molecules in the complex as well as the various steps in their thermal decomposition. The TGA thermograms were characterized by three steps, the first one within the range 50-80 ^{o}C represents the volatilization of the water molecules from the complexes. This indicates that all water molecules are present as lattice water and donot contribute to the coordination sphere. The second step within the range 90-185 ^{o}C involves the removal of acetate anions essentially as acetic acid while the third

step above 270-650 ^{o}C is due to the decomposition of the organic ligand leading to the metal oxide as a final product. The metal content of the complexes was then determined from the weight % of the remainder oxide and was found to be in a satisfactory agreement with the data of the elemental analysis and the suggested

formulae of the complexes. The DTA curves display peaks corresponding to these three thermal decomposition steps.

Table 1 : analytical and physical data of (SADH) and (DHBADH) and their metal complexes

No.	Compound	Color	M.P. (d.p.) ^{o}C	Calc. (Found) % C	H	N	H_2O	μ_{eff}
I	SADH (H_4L^1)	white	>300	62.8 (62.04)	6.39 (5.75)	14.66 (14.5)	-	
1	$[Mn_2(H_2L^1)(Ac_2O)_2]_2.H_2O$	deep yellow	>300	46.67 (46.91)	4.37 (4.5)	9.1 (9.95)	2.92 (3.55)	5.73
2	$[Co_2(H_2L^1)(Ac_2O)_2]_2.H_2O$	deep yellow	>300	46.08 (46.71)	4.32 (4.59)	8.96 (9.67)	2.88 (3.25)	1.87
3	$[Ni_2(H_2L^1)(Ac_2O)_2]_2.H_2O$	green	>300	46.1 (47.49)	4.32 (4.85)	8.96 (10.0)	2.87 (3.52)	2.05
4	$[Cu_2(H_2L^1)(Ac_2O)_2]_2.4H_2O$	green	(290)	43.5 (42.87)	4.54 (4.3)	8.47 (9.18)	5.76 (6.21)	1.05
5	$[Zn_2(H_2L^1)(Ac_2O)_2]_2.H_2O$	yellow	>300	45. 2 (46.01)	4.23 (4.2)	8.74 (7.93)	2.78 (3.66)	-
II	DHBADH (H_4L^2)	dirty White	285	57.9 (56.94)	5.31 (5.96)	13.5 (14.26)	-	-
6	$[(Mn_2(H_2L^2)(Ac_2O)_2]_2.H_2O$	Brown	(290)	44.66 (44.74)	3.72 (4.52)	10.40 (10.14)	2.73 (3.4)	5.17
7	$[(Co_2(H_2L^2)(Ac_2O)_2]_2.H_2O$	orange	>300	43.95 (43.09)	3.66 (4.50)	10.2 (9.89)	2.70 (3.01)	1.78
8	$[(Ni_2(H_2L^2)(Ac_2O)_2]_2.3H_2O$	green	>300	40.0 (40.43)	4.33 (5.15)	9.33 (10.00)	7.69 (8.15)	2.15
9	$[(Cu_2(H_2L^2)(Ac_2O)_2]_2.H_2O$	green	270	43.2 (42.87)	3.60 (4.30)	10.09 (9.81)	2.75 (3.15)	1.18
10	$[Zn_2(H_2L^2)(Ac_2O)]_2.H_2O$	yellow	>300	43.01 (42.9)	3.58 (4.01)	10.00 (10.9)	2.65 (2.15)	-

The decomposition steps can be represented as follows:

$$[M_2(H_2L)(AcO)_2].XH_2O \xrightarrow[50\text{-}80\ ^{o}C]{-XH_2O} [M_2(H_2L)(AcO)_2$$

$$[M_2(H_2L)(AcO)_2] \xrightarrow[90\text{-}185\ ^{o}C]{-2AcOH} M_2L$$

$$M_2L \xrightarrow{-L\ \ 270\text{-}650\ ^{o}C} MO$$

IR spectra

The characteristic bands in the IR spectra of the ligands H_4L^1, H_4L^2 and their metal complexes are listed in Table 2. The presence of water molecules in the

complexes is confirmed by the presence of broad bands at 3454-3400 cm^{-1} due to νOH of water molecules associated with the complex and the two weak bands around 840 and 720 cm^{-1} which can be assigned to H_2O rocking and wagging modes of vibrations[14]. In the spectra of complexes (1-9) the bands due to ν(NH) and carbonyl group νC=O (amide I) and δN-H (amide II) vibrations at 3196, 1668 and 1555 cm^{-1} of the ligand disappeared. Also new bands appeared around 1612 cm^{-1} and at 1530-1450 cm^{-1} which are assigned to the azine (νC=N-N=C) [15,16] and (νN=C-O)[17] groups respectively. This reveals the enolization of the ligand and the reaction of the enol-form with the elimination of a proton and bonding to the metal ion through both deprotonated =C-OH groups[18]. The appearance of ν(N=C-O) at 1530-1450 cm^{-1} and the shift of ν(N-N) at 1134-1165 cm^{-1}, which is observed at higher frequency than that of the free ligand and in addition, the shift of the bands at 2962-3057 cm^{-1} corresponding to νC-H of the azomethine group (N=CH-) to higher frequency on complexation confirms the coordination of the azomethine nitrogen to the metal ions[19]. This result is in accordance with the expectation that N-coordination to a metal ion having filled π-orbitals should result in a shift towards the lower energy region in the νC=N[20].

The broad intense bands of νH_2O molecule at 3400-3450 cm^{-1} make it difficult to distinguish the behaviour of the phenolic νOH band. The situation of the band corresponding to phenolic δOH and νC-OH at the same frequency of the free ligand indicates that the phenolic OH group does not participate in complex formation. The complexes are formed via bonding to the enolized carbonyl group and azomethine nitrogen thus indicating that the ligand acts as dibasic tetradentate towards each of the two metal ions in each molecule. The presence of coordinated bidentate acetate ions in the prepared complexes (1-9) is confirmed by the existence of the two bands at (1470-1434) and (1326-1386) cm^{-1} assigned to **υ** asymmetric and **υ** symmetric vibrations of the carboxylate group. The difference between the two frequencies amounts to 90-110 cm^{-1}. These values confirm the presence of bidentate bridging acetate anions[18,21,22] in the metal complexes (scheme II).

For the complex (10) the shift of νC=O to lower frequency, absence of azine group and νN=C-O group and the presence of δNH at 1540 cm^{-1} indicate that the metal ion

is coordinated to the C=O. The disappearance of δOH and shift of νC-O and νC=N to higher frequency indicate that complex formation for complex (10) takes place through deprotonation of the phenolic OH group forming covalent bond with the Zn^{2+} ion, and that the azomethine nitrogen is coordinated to Zn^{2+} ions.

Table 2: Characteristic IR, UV and ESR spectral data for (SADH) and (DHBADH) and their metal complexes

No.	νOH* νH_2O	νC=N* νC=N-N=C	νN=C-O	ν(OAC) νasy	ν(sy)	νC-O	OH (OOP) ρ ω		CT (d-d)	π-π* C=N¹ C=N²		$g_{//}$	$g_{\perp}$	g_{eff}
I	3452* (br.)H.b	1614*	-	-	-	1200				301 (354)	314 -	-	-	-
1	3425	1612	1523	1450	1335	1199	850	714	413 (492)	305	345	-	-	2.45
2	3400	1595	1530	1470	1382	1192	980	845	352 (420)	296	343	2.3	1.81	2.07
3	3412	1601	1526	1452	1339	1193	860	814	347 (389)	291	302	-	-	-
4	3425	1605	1515	1437	1326	1195	993	930	382 (435)	301	354	2.77	2.22	2.51
5	3454	1608	1532	1457	1368	1195	867	700	400	294	328	-	-	-
II	3337* (br.),H.b	1581*	-	-	-	1199	840	794		301 (325)	345	-	-	-
6	3392	1589	1498	1450	1384	1200	831	785	348 (452)	304	315	-	-	2.34
7	3410	1595	1495	1474	1382	1198	781	695	352 (420)	314	343	2.58	1.72	2.19
8	3405	1600	1481	1470	1378	1201	758	714	346 (404)	306	324	-	-	-
9	3454	1589	1505	1473	1383	1200	807	795	380 (423)	311	346	2.54	2.16	2.36
10	3400	1615*	-	1540	1395	1213	778	726	410	310	330	-	-	-

Thus the ligand acts as dibasic hexadentate ligand towards the two zinc ions. On the other hand, the difference between the two frequencies of the acetate carboxylate group lies over 154 cm^{-1} confirming the presence of unidentate acetate anions[18,21,22] for complex (10).

Electronic absorption spectra and magnetic moments

The Electronic absorption spectra of the complexes under study are summarized in Table 2. The complexes show bands in the 290-354 nm range which are attributed to π-π* intra-ligand transitions ($C=N^1$ and $C=N^2$). The formation of complexes (1-9) occurs through enolized form of the ligand and bonding to the carbonyl oxygen and azomethine nitrogen. This is confirmed by the disappearance of the band at 282-290 nm corresponding to the π-π* transitions of the C=O group from the spectra of these complexes.

The spectra of the manganese(II) complexes (1& 6) show a band in the 450-490 nm range corresponding to $^3A_1g—^3T_1g$ electronic state transition in a square pyramidal geometry[23]. The observed magnetic moment μ_{eff} for Mn^{2+} complexes (Table 1) are lower than expected for high spin d^5 complex due to the possible existence of bilateral Mn-Mn interaction.

For cobalt(II) complexes (2& 7) the band observed in the 420-430 nm range is corresponding to $^2B_2g—^2T_2g$ electronic state transition in a square planar geometry[24] for the low spin Co^{2+} complexes (2,7). The magnetic moment value 1.67 B.M. is slightly lower than the spin only value for one unpaired electron in the d-orbital in case of low spin Co^{2+} complexes which can be ascribed to the existence of Co-Co interaction in the complexes. Nickel(II) complexes (3 & 8) show a band at 385-404 nm range corresponding to $^3A_2g—^3T_1g$ electronic state transition. The magnetic moment values indicate the presence of two unpaired electrons in the d-orbital and confirm that the complex is present in tetrahedral arrangement[25,26]. The low μ_{eff} value reflects an obvious metal-metal interaction in the solid lattice.

The spectra of the copper(II) complexes (4& 9)show bands at 420-550 nm range corresponding to M-L CT and d-d transitions assigned to $^2B_1g—^2A_1g$ and $^2B_1g—^2E_1g$ electronic states in a square planar arrangement[27]. The magnetic moment value 1.05 B.M. is much lower than expected for the spin only value of one unpaired electron in the d^9 copper ion. This reflects strong Cu-Cu interaction. Zinc(II) complex (10) shows two bands at 310 and 330 nm assigned to π-π^* transitions of $C=N^1$ and $C=N^2$ indicating that complex formation occured through carbonyl oxygen and azomethine nitrogen in addition to phenolic oxygen. The band at 410 nm is assigned to an intra-molecular charge transfer. The electronic absorption spectra and the diamagnetic character of the Zn^{2+} complexes show the tetrahedral geometry[28] around the metal ion.

ESR spectra

The ESR spectra of metal chelates provide informations about hyperfine and super hyperfine structures which are important in studying the metal ion environment in the complexes, i.e. the geometry, nature of ligation from the ligand to the metal ion and the degree of covalency of the metal- ligand bonds

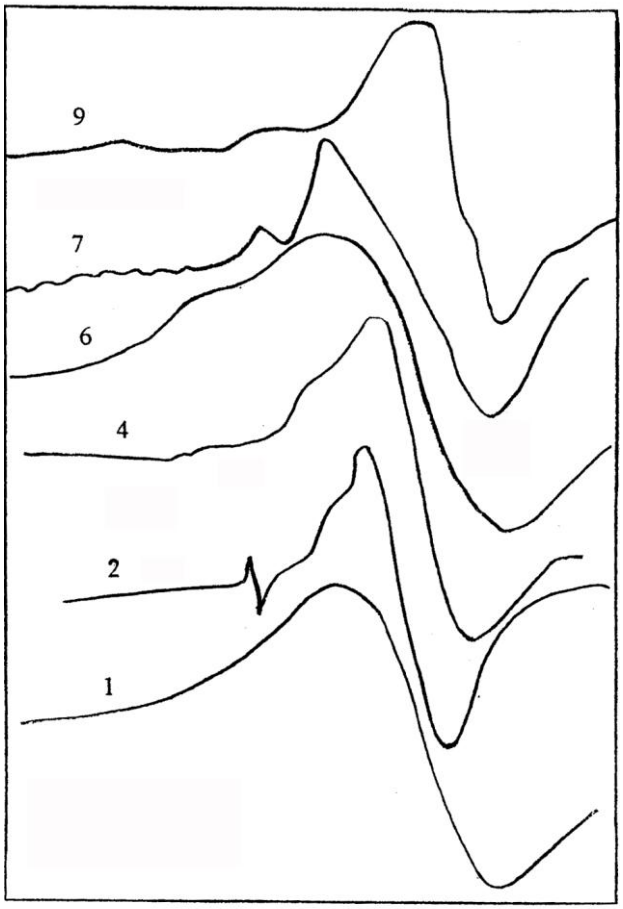

Fig. 1 : ESR spectra of metal complexes

The solid state powder X-band ESR spectra of manganese(II), cobalt(II) and copper(II) complexes were measured at room temperature (Fig. 1). The g_{eff} values are recorded in Table 2. The spectra of Mn^{2+} complexes show strong broad signals with g_{eff} values 2.45 and 2.34 for complexes (1) and (6) respectively, which are characteristic for square pyramidal high spin Mn^{2+} complex. The broadening of the signals results from spin-spin interaction between Mn^{2+} ions which confirms the data of magnetic moment indicating lateral Mn^{2+}-Mn^{2+} interaction in the binuclear complex. The positive deviation of g_{eff} from the value of the free electron 2.0023 can be due to partial increased covalent nature of the bonding between the Mn^{2+} ions and the ligand molecule[29]. The broad signal of the cobalt(II) complexes with some hyperfine structure is characteristic for ^{59}Co ions in a complex structure. The broadening of the signal results from the spin-spin interaction between the two Co^{2+} ions existing in the binuclear Co^{2+} complex which is in accordance with the results

of the magnetic moment. In the spectra of copper(II) complexes, the greater value of $g_{//}$ compared to $g_{\perp}$ indicates the presence of the unpaired electron in the ground state d_{x2-y2} orbital[30]. The g values support a square planar geometry with covalent nature of the metal ligand bonds[31]. The Cu^{2+}— Cu^{2+} exchange taking place in the copper(II) complexes is gained by the fact that no hyperfine splitting is observed as well as the value of G [$G = g_{//} -2 / g_{\perp}-2$] which equals 3.53, 3.41 for complexes (4) and (9) respectively being lower than 4[32]. This could also confirm the square planar geometry around Cu(II) ions with a significant exchange coupling present[33]. The broadening of the signal results from spin-spin interaction between the two Cu^{2+} ions existing in the binuclear Cu^{2+} complex.

Based on the previously discussed results of elemental and thermal analyses, IR spectra, magnetic moment, electronic spectra and ESR spectra , the structure of the investigated complexes can be represented as given in Scheme II.

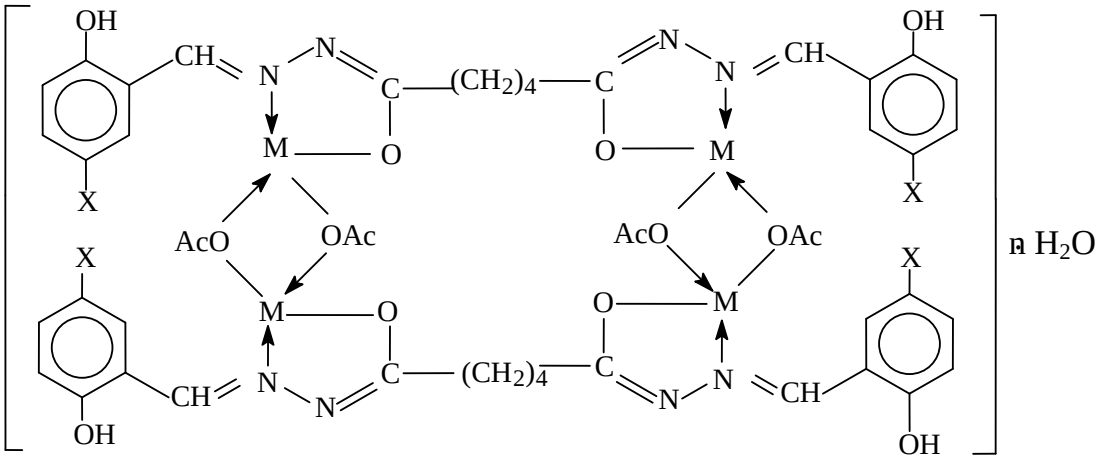

Complexes (1-9)

X= H for H_4L^1 complexes (1-5) (M and n) = (Mn, 1) for complex 1, (Co, 1) for complex 2, (Ni, 1) for complex 3, (Cu, 4) for complex 4, (Zn, 1) for complex 5.

X= OH for H_4L^2 complexes (6-10) (M and n) = (Mn, 1) for complex 6, (Co, 1) for complex 7, (Ni, 3) for complex 8, (Cu, 1) for complex 9.

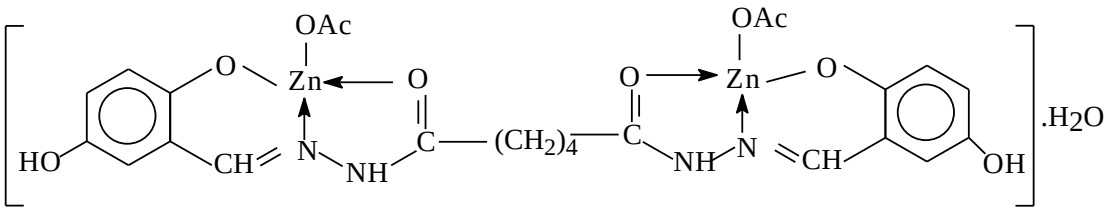

Complex (10)

Scheme II.

References

1. A.K. Sengupta and A.J. Bhatnagar, J. *Indian Chem. Soc.*, **64,** 616 (1987).
2. Aggarwal, R.C., Yaclav, B.N. and Prasad, T., *J. Inorg. Nucl. Chem.*, **35,** 653 (1973).
3. Yu.P. Kitaev, B.I. Buzykin and T.V. Troepol'skaya, *J. Chem. Soc.*, 441 (1970).
4. T.M. Tien and T.S. Ma, *Antibiotics and Chemotherapy*, **3,** 491(1953).
5. R.C. Sharma, J. Ambwani and V.K. Varshney, *J. Indian Chem. Soc.*, **69,** 770 (1992).
6. R.C. Sharma, *J. Indian Chem. Soc.*, **65,** 792 (1988).
7. J.C. Craliz , J.C. Rub, D. Willis and J. Edger, *Nature*, **34,** 176 (1955).
8. J.R. Mechant, and D.S. Clothia, *J. Med. Chem.*, **13,** 335 (1970).
9. J.A. Anten, D. Nichalls and J.M. Markopoulos, *Polyhedron*, **6,** 1075 (1987).
10. V.F. Shilgin, S.M. Zlatogorskii, V. Ya Zun and G.M. Larin, Russian Chemical Bulletin, **51**, 2273 (2002).
11. N. Manav, and N.K. Kaushik, *Transition Met. Chem.*, **27,** 849 (2002).
12. C.Li, L.weng, X.Meng, H.Zhao, Transition Met. Chem., **24**, 206 (1999)
13. A.S. El-Tabl , *Transition Met. Chem.*, **21,** 428 (1996).
14. P.R. Shukla, V.K. Singh and A.M. Jaiswal, *J. Indian Chem. Soc.*, **60,** 321 (1983).
15. M.F. Iskender, L. El-Sayed, and M.A. Lasheen, *Inorg. Chim. Acta*, **16,** 147 (1976).
16. M.S. Patil, and J.R. Saha, *J. Indian Chem. Soc.*, **58,** 944 (1981).

17. S. Ghosh and A. Maiti, *Indian J. Chem.*, **28A,** 980 (1989).
18. K. Nakamoto, "Infrared and Raman Spectra of Inorganic and Coordination Compounds". 3rd Edit., John Wiley (1978).
19. A. Baribanti, F. Dallavalli, M.A. Pellinghelli and E. Leoporati, *Inorg. Chem.*, **7,** 143 (1968).
20. R.J. Butcher, J. Josinski, G.M. Mockler and E. Sinn, *J. Chem. Soc.*, 1099 (1976).
21. G.B. Deacon and R.J. Phillips, *Coord. Chem. Rev.*, **33,** 227 (1980).
22. R. Srinivasan, I. Sougandi, K. Velavan, R. Venkatesan, V. Babu and P.S. Rao, *Polyhedron*, **23,** 1115 (2004).
23. D.M.L. Goodgame and F.A. Cotton, *J. Chem. Soc.*, 3735 (1961).
24. Y. Nishida and S. Kida, *Coord. Chem. Rev.*, **27,** 275 (1979).
25. A.M. Hammamm, S.A. Ibrahim, S.A. El-Gyar and M.M. El-Gahami, *Synth. React. Inorg. Met-Org. Chem.*, **18,** 9 (1988).
26. D.N. Kumar and B.S. Garg, *J. Therm. Anal. Cal.*, **69,** 607 (2002).
27. A.B.P.Lever, "Inorganic Electronic Spectroscopy", Elsevier, Amesterdam, 2nd Edit., (1984).
28. H. Temel, H.ren, Transition Met. Chem., **27**, 609 (2002).
29. I. Findone and K.W.H. Stevens, *Proc. Phys. Soc. London*, **73,** 116 (1959).
30. B.A. Goodwin and J.B. Raynor, *Adv. Inorg. Chem. Radio. Chem.*, **13,** 136 (1970)
31. S.N. Dubey, R.N. Handn and B.K. Vaid, *Montashefte für Chemie*, **125,** 395(1994).
32. B.J. Hathaway and D.E. Billing, *Coord. Chem. Rev.*, **5,** 143 (1970).
33. N. Raman, A. Kulanduisumy and C. Thangaraja, *Transition Met. Chem.*, **28,** 29 (2003).